Biosensors and Bioelectronics 79 (2016) 938–944

Contents lists available at ScienceDirect

Biosensors and Bioelectronics

journal homepage: www.elsevier.com/locate/bios

Gonyautoxin 1/4 aptamers with high-affinity and high-specificity: From efficient selection to aptasensor application

Shunxiang Gao [a,1], Bo Hu [a,b,1], Xin Zheng [a,c,1], Ying Cao [d], Dejing Liu [a], Mingjuan Sun [a], Binghua Jiao [a,b,*], Lianghua Wang [a,*]

[a] Department of Biochemistry and Molecular Biology, College of Basic Medical Sciences, Second Military Medical University, Shanghai 200433, China
[b] Marine Biological Institute, College of Marine Military Medicine, Second Military Medical University, Shanghai 200433, China
[c] Department of Laboratory Diagnosis, Changhai hospital, Second Military Medical University, Shanghai 200433, China
[d] Beijing Institute of Pharmaceutical Chemistry, Beijing 102205, China

ARTICLE INFO

Article history:
Received 18 November 2015
Received in revised form
28 December 2015
Accepted 11 January 2016
Available online 12 January 2016

Keywords:
In vitro selection
Optimization
Biolayer interferometry
Aptasensor

ABSTRACT

Gonyautoxin 1/4 (GTX1/4) are potent marine neurotoxins with significant public health impact. However, the ethical issues and technical defects associated with the currently applied detection methods for paralytic shellfish toxin GTX1/4 are pressing further studies to develop suitable alternatives in a regulatory monitoring system. This work describes the first successful selection, optimization, and characterization of an aptamer that bind with high affinity and specificity to GTX1/4. Compared to the typical MB-SELEX, GO-SELEX, an advanced screening technology, has significant advantages for small molecular aptamer development. Furthermore, we truncated GTX1/4 aptamer and obtained the aptamer core sequence with a higher K_d of 17.7 nM. The aptamer GO18-T-d was then used to construct a label-free and real-time optical BLI aptasensor for the detection of GTX1/4. The aptasensor showed a broad detection range from 0.2 to 200 ng/mL GTX1/4 (linear range from 0.2 to 90 ng/mL), with a low detection limit of 50 pg/mL. Moreover, the aptasensor exhibited a high degree of specificity for GTX1/4 and no cross reactivity to other marine toxins. The aptasensor was then applied to the detection of GTX1/4 in spiked shellfish samples and showed a good reproducibility and stability. We believe that this novel aptasensor offers a promising alternative to traditional analytical methods for the rapid detection of the marine biotoxin GTX1/4.

1. Introduction

According to reports, paralytic shellfish poisoning (PSP) is one of the top three global marine biological hazards (Acres and Gray, 1978). The most representative neurotoxins in paralytic shellfish toxins (PSTs) are gonyautoxin 1/4 (GTX1/4) and their analogues such as gonyautoxin 2/3 (GTX2/3), saxitoxin (STX) and neosaxitoxin (neoSTX) (Fig. S1), which have very similar structures but different toxicity (Wiese et al., 2010). GTX1 and GTX4 are epimers with special molecular structures (two guanidine groups, one sulfonic acid group) that can transform into each other in neutral or alkaline conditions until reaching an equilibrium state and thus usually coexist (Dorr et al., 2011). GTX1/4 accumulate in shellfish of various species through the aquatic food chain, and the ensuing consumption of GTX1/4-contaminated shellfish by humans causes PSP and even death (Evans, 1965). As the contamination of shellfish with GTX1/4 has adverse effects on human health as well as the global shellfish industry, multiple detection methods for marine biotoxin GTX1/4 have been developed. The mouse bioassay (MBA) standardized by the Association of Analytical Communities (AOAC) has been internationally accepted as the official reference method for the detection of GTX1/4 in shellfish (Truman and Lake, 1996). However, the low sensitivity, high cost, and ethical problem still need to be overcome. Some other analytical methods have been developed, such as high-performance liquid chromatography coupled to fluorescence or mass spectrometry, which has been approved by the European Union (EU) as a first action method for GTX1/4 detection in shellfish (Lawrence et al., 2005). However, most of these techniques are time consuming and require expensive instruments as well as toxin reference standards for accurate identification and quantification, which are difficult to

* Corresponding authors at: Department of Biochemistry and Molecular Biology, College of Basic Medical Sciences, Second Military Medical University, Shanghai 200433, China.
E-mail addresses: bhjiao@smmu.edu.cn (B. Jiao), lhwang@smmu.edu.cn (L. Wang).
[1] Co-first authors.

http://dx.doi.org/10.1016/j.bios.2016.01.032
0956-5663/

obtain. Therefore, the development of a sensitive, robust and inexpensive monitoring system for the detection of GTX1/4 in shellfish is urgently needed. Biosensors are ideal alternatives for the monitoring of marine biotoxins because they can make up for most of the shortcomings of other methods. To date, there are no reports on biosensors for GTX1/4 detection because there is no identified specific recognition molecule, such as an antibody, that can bind to GTX1/4.

Aptamers are functional single-stranded DNA or RNA fragments screened from a random oligonucleotide library through an *in vitro* evolution-like process known as Systematic Evolution of Ligands by Exponential Enrichment (SELEX) (Ellington and Szostak, 1990). Since the aptamer concept was first proposed by Tuerk et al. in 1995 (Tuerk and Gold, 1990), the *in vitro* screening technique for aptamers, SELEX, has been greatly improved, and numerous aptamers with high affinity and specificity for various targets have been successfully identified and adopted as diagnostic or analysis tools (Germer et al., 2013). While antibodies are the most popular biomaterial for molecular recognition elements, having been developed as molecular recognition probes as early as the 1950s, aptamer, as potential, stable and low cost recognition reporters which can replace antibodies is used to bioassay (Jayasena, 1999). Currently, aptamers as molecular recognition probes can be used to constructed a variety of biosensor, such as biolayer interferometry (BLI), surface plasma resonance (Cao et al., 2011), quartz crystal microbalance (Song et al., 2014) or electrochemical methods (Ferapontova et al., 2008). However, BLI is a promising sensing platform because it provides a label-free, highly sensitive, cost-effective and real-time optical biosensor, especially suitable for the on-site rapid analysis of marine biotoxins.

Although several aptamers have been selected that target marine biotoxins, including brevetoxin-2 (Eissa et al., 2015), okadaic acid (Eissa et al., 2013), Microcystin-LR (Ng et al., 2012) and saxitoxin (Handy et al., 2013; Zheng et al., 2015) with high affinity and specificity, there have been no reports of aptamer screening and identification for GTX1/4, mainly because of the great challenges in small molecular aptamer development. Recently, a novel and versatile screening technique for aptamer development, GO-

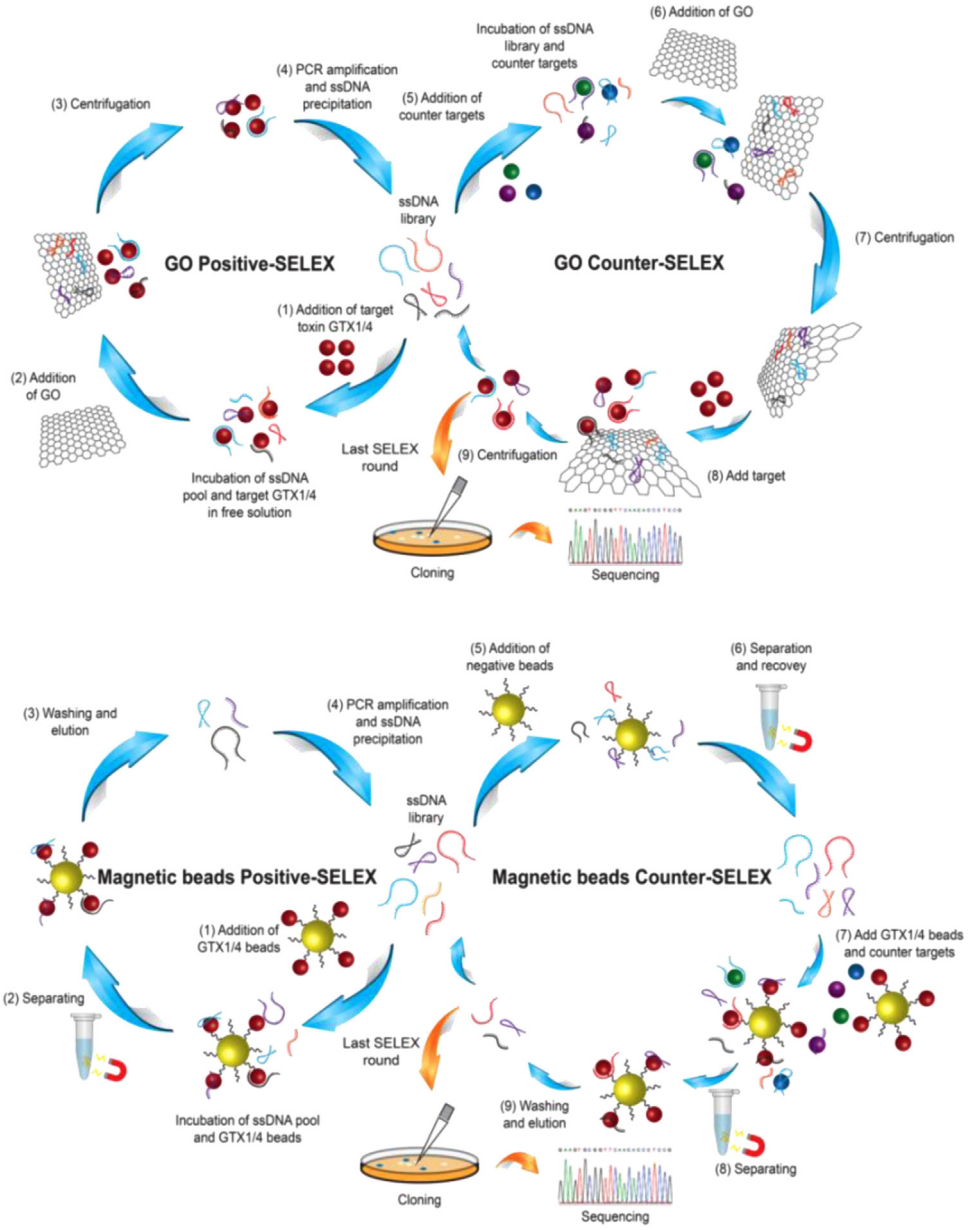

Fig. 1. Aptamer Selection Process: GO-SELEX (top) and MB-SELEX (bottom).

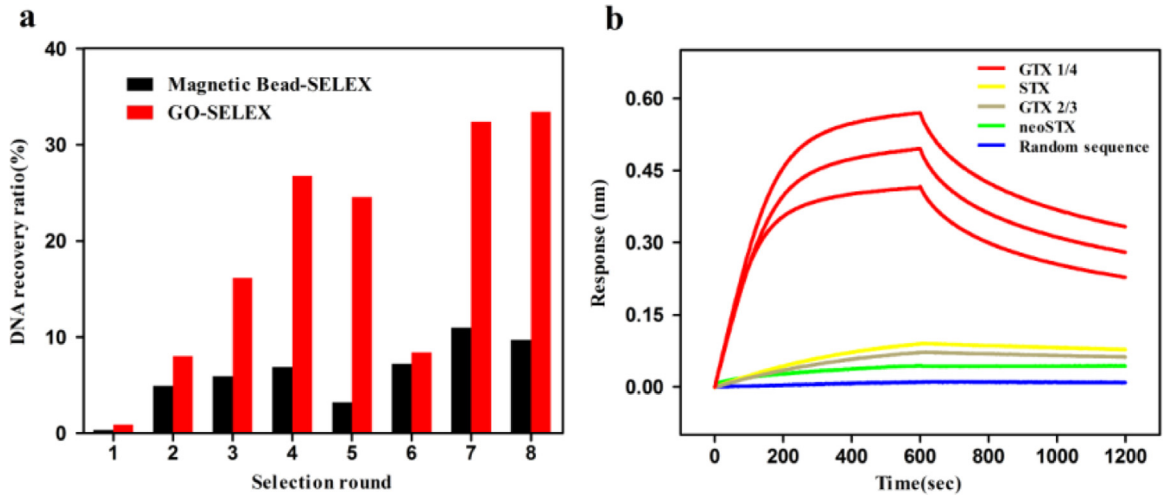

Fig. 2. (a) Enrichment of GTX1/4 binding ssDNA during MB-SELEX and GO-SELEX. The red bar graph shows the amount of ssDNA recovered from the GO-SELEX supernatant in each selection round. The black bar graph shows the amount of ssDNA eluted from GTX1/4 beads in each selection round. (b) Characterization of affinity and specificity of aptamer GO18-T-d for GTX1/4. The reddish-brown lines represent the interaction curve of aptamer GO18-T-d with GTX1/4 (20 μM (top), 10 μM (middle), and 5 μM (bottom)). The blue line represents the interaction curve of a random sequence with GTX1/4. The yellow, gold, and green lines represent the interaction curves of aptamer GO18-T-d with STX, GTX2/3, and neoSTX, respectively.

SELEX, has attracted researchers' attention (Park et al., 2012). It is an graphene oxide-based screening method, which is immobilization-free, highly efficient and cost-effective.

In this study, two independent SELEX experiments were conducted targeting marine biotoxin GTX1/4, one using the novel GO-SELEX and the other using a typical MB-SELEX (Fig. 1). Compared to the typical MB-SELEX, GO-SELEX has significant advantages for small molecular aptamer development. In addition, we carried out GTX1/4 aptamer optimization and obtained its core sequence with a higher K_d of 17.7 nM. The aptamer GO18-T-d was then used as a novel molecular recognition element to construct a simple, label-free and real-time optical BLI aptasensor for the detection of GTX1/4. This novel aptasensor is promising and offers an alternative to the traditional analytical methods for the rapid and simple detection of marine biotoxin GTX1/4.

2. Materials and methods

All the materials, reagents, experimental methods and instrumentations used throughout this study are described in details in the Supporting information.

2.1. In vitro selection of the DNA aptamer

The selection of the aptamers against GTX1/4 was performed according to the process described in Fig. 1. Aptamer screening protocol and binding analysis of the selected sequences were performed as explained in details in the Supporting information.

2.2. Determination of affinity and specificity of aptamer GO18-T-d by BLI

The affinity and specificity of aptamer GO18-T-d were determined by BLI using an OctetRED 96 system (ForteBio, Shanghai). The principle and analysis procedures used herein were as detailed in Concepcion et al. (2009). As shown in Fig. S6, the assay procedure includes five steps: (1) baseline (2 min); (2) loading (5 min); (3) washing (3 min); (4) association (10 min); (5) baseline (10 min). The baseline solution (A, 200 μL, 20 mM Tris–HCl, 100 mM NaCl, 2 mM $MgCl_2$, 5 mM KCl, pH 7.5), loading solution (B, i.e. baseline solution), washing solution (C, i.e. baseline solution), association solution (D, i.e. baseline solution) and dissociation solution (E, i.e. baseline solution) were respectively added into the corresponding wells in a 96-well microtiter plate (Fig. S6A). The response data obtained from the reaction surface were normalized by subtracting the signal simultaneously acquired from the control surface to eliminate nonspecific binding and buffer-induced interferometry spectrum shift using the Octet Data Analysis Software CFR Part 11 Version 6.x; the affinity parameter K_d was then obtained. A 1:1 binding mode with mass transfer fitting was used to obtain the kinetic data.

3. Results and discussion

3.1. GTX1/4 aptamer selection

3.1.1. GO-SELEX

GO-based SELEX includes positive-selection rounds and counter- selection rounds, as illustrated in Fig. 1. In the GO positive-selection process, the random ssDNA library was incubated with the target toxin GTX1/4 and the GO solution. The ssDNA that could not bind to the target was absorbed on the GO surface, while the ssDNA that could bind to the target remained in solution in the form of aptamer-toxin complexes. In the separation procedure, the deposits as well as the ssDNA that were adsorbed on the GO surface through π-π stacking and hydrophobic interactions were discarded by centrifugation, while the ssDNA bound to the target in the supernatant was recovered and amplified. With the ssDNA recovery ratio significantly increasing (Fig. 2a), counter-selection was introduced after round 5 to eliminate false-positive binding of aptamers to toxins that were similar to the target. In the GO counter-selection process, the counter targets (GTX2/3, STX and neoSTX) were first incubated with the ssDNA pool. Then, the mixture was added to the GO solution for further incubation, and the ssDNA adsorbed on the surface of the GO at this stage was likely potential aptamers specifically binding the target toxin. During affinity-based competitive capture, when the target was infinitely close to the potential aptamers adsorbed on the GO surface, the target was capable of inducing a conformational change in the aptamer candidates. The adaptive refolding of the aptamer to a unique three-dimensional structure that specifically bound to the target in turn broke the π–π stacking and

hydrophobic interactions between the aptamers and GO, resulting in aptamer release from the GO surface. After 8 rounds of selection (Fig. 2a), the ssDNA recovery ratio was found to be similar to the previous (7th) round, which indicated that the binding sites on the target in the system had almost reached saturation. The selection cycles were stopped, and the enriched ssDNAs were cloned and sequenced.

3.1.2. MB-SELEX

We immobilized GTX1/4-carboxylated derivative on M-270 Amine Dynabeads through the coupling reaction between the carboxy groups on the toxin and the amino groups on the beads via the EDC/NHS chemistry (Fig. S2). The rest of the amino groups on the beads were blocked with propionic acid to reduce the non-specific binding of the beads to ssDNA. The bead-based screening process, including positive selection and counter selection, is illustrated in Fig. 1 following the protocol detailed in Table S1. From round 2, the negative beads were introduced to remove the ssDNA that bound non-specifically to the magnetic beads to improve the screening efficiency. From round 3, free competitive counter-molecules were added in the positive incubation system to improve the specificity of screening. After 8 rounds of selection (Fig. 2a), the ssDNA recovery ratio had significantly increased and reached a plateau. The selection cycles were also stopped, and the enriched ssDNAs were cloned and sequenced.

The GO-SELEX and MB-SELEX each identified 40 sequences. After multiple sequence alignment and secondary structure prediction, the alternative aptamers were divided into similar families (Fig. S3 and S4) based on sequence conservation. Then, the sequence with the highest homology or minimum free energy in each group was chosen for further binding affinity studies with GTX1/4, as shown in Table S2. For the sequences obtained by GO-SELEX screening, six aptamers showed high affinity for the target, ranging from 62.0 to 653 nM, while two sequences showed no binding. However, the aptamers obtained by MB-SELEX exhibited almost no binding to GTX1/4, and only three sequences were capable of binding the target with K_d in the micromolar range. Throughout the screening process, we maintained the consistency of both *in vitro* selection methods to the greatest extent, but GO-SELEX exhibited higher efficiency. First, each round of recovery of ssDNA in the GO-SELEX process was significantly higher than in MB-SELEX (Fig. 2a). Second, the sequences obtained by GO-SELEX showed high homology, with multiple repetitive sequences among them (Fig. S3), while the sequences obtained by MB-SELEX had low homology with almost no repetitive sequences (Fig. S4). Last and most importantly, the aptamers selected by GO-SELEX exhibited higher affinity in the nanomolar range, while the aptamers selected by MB-SELEX had relatively low affinity ranging from tens of μM to several μM, with a gap up to 100-fold (Table S2). Although aptamers with similar affinity might be discovered through further selection by MB-SELEX, GO-SELEX is not only more efficient in screening but also easier to operate without relying on special equipment. Moreover, conformational changes to the targets and interference from the binding of the pool to the conjugation side of the targets were avoided because there is no need for target immobilization in the GO-SELEX process. Therefore, GO-SELEX is a simplified, high-speed and immobilization-free method for aptamer screening, and it provides an alternative novel method for small-molecule DNA aptamer development in particular.

3.2. Truncation of aptamer GO18

In addition to a whole selection process, we also optimized aptamer GO18, which showed the highest affinity. All truncated sequences are shown in Table S3, with their secondary structures predicted by the mfold program (Fig. S5). After the primers at both ends of GO18 were truncated, GO18-T not only showed the capability of binding to GTX1/4 but also exhibited good affinity. We then further truncated stem-loop a, b or c of GO18-T separately based on the secondary structure. The affinity binding experiments revealed that GO18-T-a exhibited higher binding affinity to GTX1/4, while GO18-T-b and GO18-T-c showed no binding. This result indicated that the stem-loop structures b and c in GO18-T specifically bind to the target through the formation of a unique spatial structure. When stem-loop a was removed, the affinity of GO18-T-a for GTX1/4 increased, possibly because the binding sites for GTX1/4 on stem-loops b and c were exposed after the truncation of stem-loop a, so that the aptamer could more compactly entwine and wrap around GTX1/4. Therefore, we further removed inactive nucleotides from GO18-T-a and obtained the core aptamer sequence GO18-T-d with a K_d of 21.9 nM, which consisted of only 25 nucleotides.

3.3. Identification of affinity and specificity of aptamer GO18-T-d

As shown in Fig. 2b, different concentrations of GTX1/4 (20 μM, 10 μM, and 5 μM) were analyzed for association and dissociation, along with 5 μM GTX2/3, STX, and neoSTX as non-specific targets as well as a blank sample containing only running buffer for reference. Moreover, a random sequence was used as an aptamer control. The results revealed that GTX1/4 interacted with GO18-T-d with a K_{on}(1/Ms) value of 6.43E+04, a K_{dis}(1/s) value of 1.14E-03 and a K_d (M) value of 1.77E-08. In addition, the random sequence showed no binding to GTX1/4, which demonstrated that GTX1/4 only bound specifically to GO18-T-d. At the same time, GTX1/4 congeners, including GTX2/3, STX, and neoSTX, caused no response, which revealed that GO18-T-d only specifically bound to GTX1/4. The results of BLI (K_d=17.7 nM) and binding affinity assays (K_d=21.9 nM) showed a high degree of consistency and indicated that aptamer GO18-T-d bound to GTX1/4 with high affinity and specificity.

3.4. BLI aptasensor for GTX1/4 detection

The GTX1/4 aptamer (GO18-T-d) was then used to fabricate a label-free, real-time optical aptasensor based on BLI detection. BLI is an innovative, powerful biosensor platform that that handles samples without micro fluidics, which utilizes biolayer interferometry technology to monitor the changes in the interfacial properties at the sensor surface upon biological binding events (Hong et al., 2012). As shown in Fig. S7 (Concepcion et al., 2009), when aptamers were immobilized on sensors surface, a shift can be determined in the interference spectrum and recorded as a change in wavelength as a function of time. The wavelength shift ($\Delta\lambda$, Fig. S7) is used as a direct measurement covering the change in the optical thickness and mass density of the sensor layer. When target molecule GTX1/4 binding to or dissociating on the biosensor surface could change the interference spectrum and generate response curves. The interference, as a characteristic spectral signature, is captured and is recorded in relatively intensity units. Our online constructed three-chip sensors include SSA, SA and AR2G sensors. As shown in Fig. 3a, the SSA aptasensor response was significantly higher than the response of the other two sensors when interacting with GTX1/4 at the concentration of 500 ng/ml. This difference is mainly because more aptamers can be immobilized on the spatial structure of the SSA sensor chip, resulting in a greater mass density change on the biolayer surface. Most notably, the three-dimensional conformation of the aptamer changes significantly upon binding to GTX1/4 and results in a larger increase in the biolayer thickness. Therefore, a SSA sensor chip, which showed the greatest response, was successfully

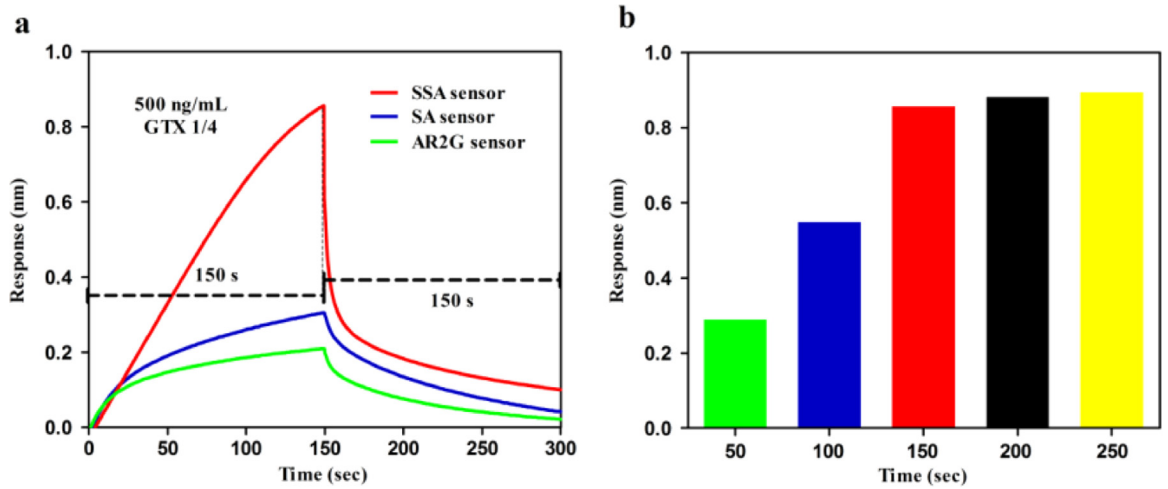

Fig. 3. (a) Response curves of different aptasensors after the addition of 500 ng/mL GTX1/4. (b) The effect of incubation time on GTX1/4-aptamer binding, monitored by measuring the response after incubating the SSA aptasensor with 500 ng/ml GTX1/4.

prepared as a GTX1/4 aptasensor. To further optimize the aptasensor, we obtained insight into the factors that might influence the interaction between aptamer GO18-T-d and GTX1/4. The binding time, sodium, magnesium and potassium ion concentrations and the pH of the binding buffer were all studied. Fig. 3b displays the GTX1/4 aptasensor's response data over time after the addition of 500 ng/ml GTX1/4. A continued enhancement of the response was observed until 150 s, when saturation was reached. Therefore, 150 s was chosen as the optimum binding time in the following experiments.

Fig. 4a reveals that the aptasensor signal is strongly dependent on Mg^{2+} concentration, which is consistent with previous reports on other aptamers (Cruz-Aguado and Penner, 2008). A continued increase in the aptasensor signal with increasing magnesium ion concentration was observed, and after the Mg^{2+}concentration reached 10 mM, no significant change occurred. These results suggest that the magnesium ions could affect the conformation of aptamer GO18-T-d and assist the formation of the toxin–aptamer complex. However, when the concentration of other cations in the binding buffer was changed, almost no effect was observed on the aptamer binding with its target (data not shown).

Fig. 4b shows the influence of pH on toxin–aptamer binding as monitored by the aptasensor response. A significant impact on the aptamer-toxin binding was observed at pH 2.5 and pH 11.5. However, there was no significant change in the aptasensor response for pH 5.0–9.0. To better understand the origin of this effect, CD spectra (Fig. 4c) results were obtained, which showed a characteristic positive spectral peak at 295 nm and a negative spectral peak at approximately 265 nm, indicative of the G-quadruplex signature. The structural stability of the aptamer with the G-quadruplex decreases when the pH deviates from 7.5, leading to a significant change in the intensity of the CD spectral peak. In particular, at pH 11.5, a strongly alkaline condition, the structure of the aptamer with G-quadruplex was completely denatured, resulting in a loss of interaction between the aptamer and toxin. In addition, the response data from BLI as well as the CD spectra also changed significantly along with pH in acidic conditions, which confirmed the important role of pH in the structural stability of the DNA aptamer. Therefore, the detection time of 300 s and the optimized binding buffer, which consists of 20 mM Tris–HCl and 10 mM $MgCl_2$ at pH 7.5, were adopted for subsequent experiments to improve the aptamer-toxin binding affinity and enhance the signal of the aptasensor. Under these optimized conditions, we determined the binding affinity of the GTX1/4 aptamer again and obtained a K_d value of 8.1 nM.

To utilize this BLI aptasensor for GTX1/4 detection, we evaluated the properties of this biosensor. Its real-time responses in the optimized condition to GTX1/4 at different concentrations, ranging from 0.2 to 200 ng/mL, were observed. As shown in Fig. 5a, the BLI response rose with increasing GTX1/4 concentration due to the larger density and thickness change of the biolayer surface. A calibration curve of the BLI responses at 150 s against GTX1/4 concentration was drawn, with each sample detected in triplicate (Fig. 5b), and then fitted to a sigmoidal logistic five-

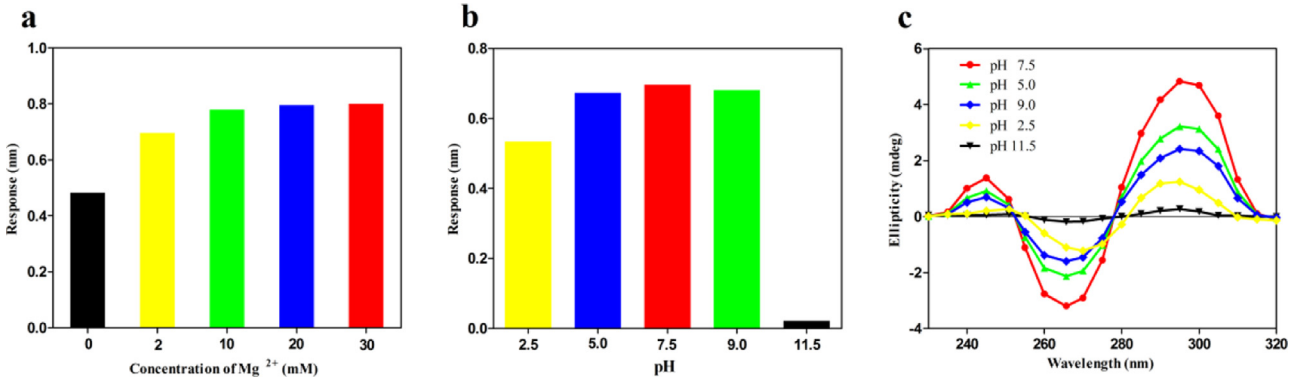

Fig. 4. (a) Effects of different Mg^{2+} concentrations on SSA aptasensor response after incubating the aptasensor with 200 ng/mL GTX1/4. (b) Effects of different pH values of binding buffer on SSA aptasensor response after incubating the aptasensor with 200 ng/mL GTX1/4. (c) CD spectra of the GTX1/4 and aptamer binding in binding buffer at different pH values.

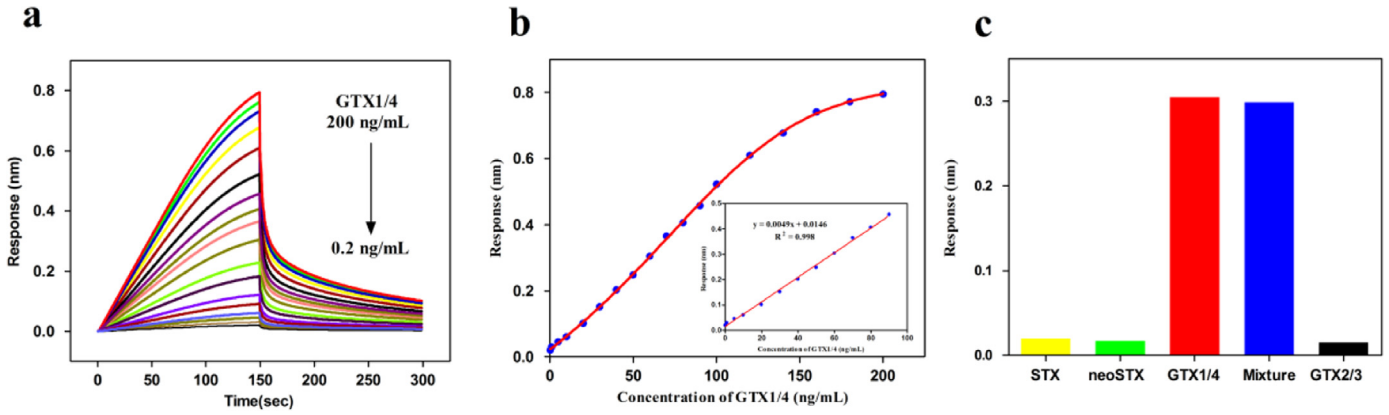

Fig. 5. (a) Response plot for the aptamer-based BLI biosensor after addition of GTX1/4 at different concentrations (0.2–200 ng/mL). (b) The calibration curve for GTX1/4, plot of Response vs. GTX1/4 concentration. Data points are the average ± one standard deviation (n=3, LOD=0.05 ng/mL, S/N=3). (c) Specificity of the aptasensor with STX, neoSTX, GTX1/4, GTX2/3 (each at 60 ng/ml) and the mixture (GTX1/4 at 60 ng/ml and other toxins each at 6000 ng/mL), separately.

parameter equation:

$$y = (R_{max} - R_{min})/[(1 + (x/EC50)\text{^}b)]\text{^}n + R_{min} \quad (1)$$

Here, R_{max}, R_{min} are the maximum and minimum response, respectively. *EC50* is the GTX1/4 concentration leading to 50% of the maximum response, b is the slope of the curve, and n is the correction factor. After the generation of the experimental data, we obtained the equation:

$$y = (0.836–0.0251)/[(1 + (x/151.398)\text{^} - 4.967)]\text{^}0.231 + 0.0251 \quad (2)$$

The correlation coefficient R^2 is 0.999. Moreover, the biosensor displayed a good linear detection range from 0.2 to 90 ng/mL of GTX1/4, which can be represented by the linear regression equation:

$$y = 0.0049x + 0.0146 \quad (3)$$

As shown in Fig. 5b, the linear plot with a regression coefficient of 0.998 was obtained. The limit of detection (LOD) was calculated to be 0.05 ng/mL(S/N=3), where the noise level is the standard deviation of multiple measurements on blank samples (n=10). The detection limit is significantly lower than the detection limit of HPLC (LOD=25 ng/ml), which is standardized by the Association of Analytical Communities (AOAC), as well as other reported detection methods. The repeatability of the aptasensor was also evaluated by measuring the signals after the addition of 60 ng/ml GTX1/4 eight times. The coefficient of variation (CV) was 1.2%, which demonstrated the good reproducibility of the aptasensor.

For practical application, good specificity of the aptasensor is a critical property in the presence of interference. Cross-reactivity experiments with GTX2/3, STX and neoSTX, which were analogs of GTX1/4, were conducted with 60 ng/mL of each toxin added. As shown in Fig. 5c, GTX1/4 caused a response of 0.32, significantly higher than the other toxin samples, which caused responses of less than 0.01. Furthermore, a toxin mixture with other toxins present in addition to GTX1/4, including GTX2/3, STX, and neoSTX (each at 6,000 ng/mL, 100 times higher than GTX1/4), yielded a signal of 0.31, which was comparable to the case when only GTX1/4 was added (0.32). These results demonstrate that GTX1/4 can be detected with good sensitivity even in a complex toxin mixture, which indicates that the aptasensor is highly specific for GTX1/4 detection.

3.5. Detection of GTX1/4 in shellfish samples

To assess the feasibility of GTX1/4 detection via the BLI aptasensor in complex matrix samples, spiked shellfish extracts were analyzed. GTX1/4 was spiked in shellfish samples with final concentrations of 5, 30 and 60 ng/mL. As shown in Table S4, a good recovery percentage of 86.70–101.29% was obtained. At the same time, the responses also indicate that non-significant interference from the shellfish matrix on the aptasensor as well as the CV value were both acceptable. Thus, we can conclude that the aptasensor possesses promising features for practical use in real sample analysis.

4. Conclusion

In conclusion, this work is the first report of successful selection, optimization and identification of DNA aptamers that bind with high affinity and specificity to GTX1/4. Compared to typical MB-SELEX, GO-SELEX, a novel screening technology, has significant advantages for small-molecule aptamer development. Furthermore, we truncated GTX1/4 aptamer and obtained the aptamer core sequence with a higher K_d of 17.7 nM.

The aptamer GO18-T-d was then used to construct a label-free and real-time optical BLI aptasensor for the detection of GTX1/4. The aptasensor exhibits a good linear range of GTX1/4 ranging from 0.2 to 90 ng/mL, with a low detection limit of 50 pg/mL. Moreover, the aptasensor showed no cross-reactivity with GTX2/3, STX and neoSTX, which are structural analogues of GTX1/4. Importantly, the aptasensor can be readily regenerated by alkaline denaturation or washing. Although the sensor is used repeatedly up to 5 times, the detection system remains stable. Furthermore, the aptasensor was applied to the detection of GTX1/4 in spiked shellfish samples and showed a good reproducibility and stability. We believe that the developed aptasensor is promising and offers an alternative to the traditional analytical methods for the rapid and simple detection of marine biotoxin GTX1/4. However, the complex structures and binding mechanism of GO18-T-d and ligands needs to be further study. In addition, several other toxin aptamers such as STX, GTX2/3 and neoSTX will be obtained in the future and will be used as the novel molecular recognition probes to construct a high-throughput and real-time optical BLI aptasensor for the detection of PSTs.

Acknowledgment

The authors would like to thank Professor Wang and Professor Fan for guidance and review of the manuscript, and National High-Tech Research and Development Program of China for the funding

for this work (2013AA092904).

Appendix A. Supplementary material

Supplementary data associated with this article can be found in the online version at http://dx.doi.org/10.1016/j.bios.2016.01.032.

References

Acres, J., Gray, J., 1978. Can. Med. Assoc. J. 119, 1195–1197.
Cao, S.H., Xie, T.T., Cai, W.P., Liu, Q., Li, Y.Q., 2011. J. Am. Chem. Soc. 133, 1787–1789.
Concepcion, J., Witte, K., Wartchow, C., Choo, S., Yao, D., Persson, H., Wei, J., Li, P., Heidecker, B., Ma, W., Varma, R., Zhao, L.S., Perillat, D., Carricato, G., Recknor, M., Du, K., Ho, H., Ellis, T., Gamez, J., Howes, M., Phi-Wilson, J., Lockard, S., Zuk, R., Tan, H., 2009. Comb. Chem. High Throughput Screen. 12, 791–800.
Cruz-Aguado, J.A., Penner, G., 2008. J. Agric. Food Chem. 56, 10456–10461.
Dorr, F.A., Kovacevi, B., Maksi, Z.B., Pinto, E., Volmer, D.A., 2011. J. Am. Soc. Mass. Spectrom. 22, 2011–2020.
Eissa, S., Ng, A., Siaj, M., Tavares, A.C., Zourob, M., 2013. Anal. Chem. 85, 11794–11801.
Eissa, S., Siaj, M., Zourob, M., 2015. Biosens. Bioelectron. 69, 148–154.
Ellington, A.D., Szostak, J.W., 1990. Nature 346, 818–822.
Evans, M.H., 1965. Br. J. Exp. Pathol. 46, 245–253.
Ferapontova, E.E., Olsen, E.M., Gothelf, K.V., 2008. J. Am. Chem. Soc. 130, 4256–4258.
Germer, K., Leonard, M., Zhang, X., 2013. Int. J. Biochem. Mol. Biol. 4, 27–40.
Handy, S.M., Yakes, B.J., DeGrasse, J.A., Campbell, K., Elliott, C.T., Kanyuck, K.M., Degrasse, S.L., 2013. Toxicon 61, 30–37.
Hong, Y., Muenzner, J., Grimm, S.K., Pletneva, E.V., 2012. J. Am. Chem. Soc. 134, 18713–18723.
Jayasena, S.D., 1999. Clin. Chem. 45, 1628–1650.
Lawrence, J.F., Niedzwiadek, B., Menard, C., 2005. J. AOAC Int. 88, 1714–1732.
Ng, A., Chinnappan, R., Eissa, S., Liu, H., Tlili, C., Zourob, M., 2012. Env. Sci. Technol. 46, 10697–10703.
Park, J.W., Tatavarty, R., Kim, D.W., Jung, H.T., Gu, M.B., 2012. Chem. Commun. 48, 2071–2073.
Song, W., Zhu, Z., Mao, Y., Zhang, S., 2014. Biosens. Bioelectron. 53, 288–294.
Truman, P., Lake, R.J., 1996. J. AOAC Int. 79, 1130–1133.
Tuerk, C., Gold, L., 1990. Science 249, 505–510.
Wiese, M., D'Agostino, P.M., Mihali, T.K., Moffitt, M.C., Neilan, B.A., 2010. Mar. Drugs. 8, 2185–2211.
Zheng, X., Hu, B., Gao, S.X., Liu, D.J., Sun, M.J., Jiao, B.H., Wang, L.H., 2015. Toxicon 101, 41–47.